Check for updates

A thermodynamic modeling of 2-bed adsorption desalination to promote main equipment performance

Amirhossein Amirfakhraei, Jamshid Khorshidi and Taleb Zarei

ABSTRACT

Adsorption desalination utilizes the discrete adsorption of the water vapor from the evaporator, and is capable of being discharged to the condenser. This study illuminated an advanced cycle of mass and heat recovery among beds, condensers, and evaporators. Morover, the thermodynamic modeling of adsorption desalination systems (ADS) under different operating conditions was investigated. Furthermore, its effect on the evaporator vapor production and the water vapor adsorption and desorption in the adsorption beds were accounted for. Parenthetically, the mathematical model of ADS thermodynamics was validated with the experimental data. Besides, the advanced ADS modeling was conducted via mass and heat recovery among beds, condensers, and evaporators. In addition to the amount of desalinated water, the time history chart of the equipment applied in the process with and without the thermal and mass recovery is also illustrated. Finally, under such operating conditions, the specific daily water production (SDWP) advanced ADS is 153% higher than conventional ADS.

Key words | adsorption, desalination, heat recovery, mass recovery

Amirhossein Amirfakhraei
Jamshid Khorshidi (corresponding author)
Taleb Zarei
Department of Mechanical Engineering,
University of Hormozgan,
Bandar Abbas,
Iran
E-mail: *khorshidi@hormozgan.ac.ir*

HIGHLIGHTS

- A new ADS with recovery mode has been proposed.
- Effect of recovery mode on evaporation rate is investigated.
- Effect of recovery mode on vapor adsorption and desorption is investigated.
- Using the recovery mode increases the SDWP by 153%.

INTRODUCTION

Lack of water is due to the lack of freshwater resources to meet water needs. This problem affects all continents, and in 2019 it was cited by the World Economic Forum as one of the largest global threats in terms of its potential impact over the next decade. The lack of water is exacerbated by economic competition for the water quantity or quality, consumer disparities, irreversible depletion of groundwater, and adverse environmental impacts (Thomas 1994; Miller 2003; Trenberth *et al.* 2007; Tlili *et al.* 2019). The World Health Organization (WHO) estimates that 783 million people lack access to clean water and 2.5 billion have limited access (Kaldellis & Kondili 2007; Hulton & WHO 2012), while many people are left without access to basic levels of drinking water and sanitation. The best solution to remedy this deficiency is to apply clean technologies for water desalination. Water desalination separates dissolved salts and other minerals from the water (Gleick 1993; De Villiers 2001;

This is an Open Access article distributed under the terms of the Creative Commons Attribution Licence (CC BY 4.0), which permits copying, adaptation and redistribution, provided the original work is properly cited (http://creativecommons.org/licenses/by/4.0/).

doi: 10.2166/wrd.2021.059

Downloaded from http://iwaponline.com/jwrd/article-pdf/11/1/136/842416/jwrd0110136.pdf
by guest

Garg *et al.* 2019; Kariman *et al.* 2019; Seyednezhad *et al.* 2020).

Different desalination processes have been developed, some of which are currently under research and development. The two main technologies used mainly for desalination are thermal and membrane desalination. Thermal desalination is one of the oldest methods of sea desalination. Since this technology is more expensive than adsorption desalination technology (Youssef *et al.* 2014), it can be a good alternative to this technology for making new desalination plants. The technology is based on the principles of evaporation of the seawater which then condensates the vapor collection to obtain pure water. Membrane desalination uses a permeable membrane to transfer water or salt to two zones with different concentrations for freshwater production. The most important process in desalination deals with reverse osmosis (RO) membrane. The RO procedure consists of four main processes: (1) pre-treatment process; (2) high pressure pumps; (3) membrane process; and (4) post-treatment (Trenberth *et al.* 2007; Karagiannis & Soldatos 2008; Navarro 2018; Sabiri *et al.* 2018; Sadi *et al.* 2019; Xu *et al.* 2019; Zarei & Behyad 2019; Zhu *et al.* 2019; Amirfakhraei *et al.* 2020).

The concept of the adsorption desalination cycle differs from conventional desalination since it involves hydrophilic adsorbents. Adsorption desalination enjoys several advantages, including (Amirfakhraei *et al.* 2020): (1) it requires low temperature heat so it can use the waste heat in industries as a heat source; (2) maintenance costs are very low because there are only a few moving parts; (3) due to low operating temperature and pressure, it causes low scaling and corrosion; (4) the produced water is of very high quality; (5) it is capable of producing cooling simultaneously with the production of desalinated water. Recently, a large number of studies have been conducted in the realm of adsorption desalination. Recent adsorption desalination systems (ADS) improvements are listed in Table 1. Thu *et al.* (2011, 2013a, 2013b) and Ng *et al.* (2013) studied the performance of the adsorption desalination system with silica gel adsorbent to produce desalinated water and cooling power. Also, they investigated the effect of cooling water and hot water temperature, condenser and evaporator temperature and cycle time with respect to the cycle performance parameters. Besides, they investigated the two- and four-bed absorption desalination system. In the two-bed system, the amount of water produced is 7.4 m^3/ton of silica gel/day, and in the four-bed system, the amount of water produced is 8.9 m^3/ton of silica gel/day. Ali & Chakraborty (2016) investigated the adsorption desalination system via zeolite and silica gels as adsorbents. The system consists of two stages as well as two evaporators, which transfer the heat from the condenser to the evaporator. The amount of water produced in this system was 5% higher than the conventional systems. Shahzad *et al.* (2014) investigated a multi-effect hybrid adsorption desalination system. They showed that this hybrid system could produce 300% more desalinated water than conventional systems. Wang *et al.* (2007) experimentally investigated an adsorption desalination system, and functional experiments were performed with and without heat and mass recovery methods. Experiments show that these methods can increase the specific water production ratio and yield of freshwater plants by 15.7 and 42.5%, respectively. Youssef *et al.* (2015a, 2015b, 2016) examined the configuration of the new ADS cycle with an integrated condenser-evaporator. The new ADS design includes four beds, i.e. one evaporator, one condenser, and one enclosed evaporator-condenser unit. Also, Thu *et al.* (2013a, 2013b, 2013c, 2013d, 2013e, 2014) investigated the performance of ADS with different modes of heat recovery. They studied the heat recovery of the condenser to the

Table 1 | Constant parameters in linear driving force (LDF) model

Ref.	Working pairs	$D_{so}(m^2/s)$	$E_a(J/mol)$	R_p(m)	$f_0(constant)$
Alsaman *et al.* (2017)	Silica-gel blue/water	2.25×10^{-10}	515.97	1.75×10^{-3}	32
Tokarev *et al.* (2002), Zhu *et al.* (2006), Wang *et al.* (2014)	Silica gel CaCl2/water	2.54×10^{-4}	42,000	1.74×10^{-4}	15
Thu *et al.* (2013c)	RD silica-gel water	2.54×10^{-4}	42,000	1.7×10^{-4}	15

Downloaded from http://iwaponline.com/jwrd/article-pdf/11/1/136/842416/jwrd0110136.pdf
by guest

evaporator and vice versa as well as the integrated condenser-evaporator. In this scheme, the evaporation temperature increases due to the heat recovery from the condenser. In addition, increasing the evaporator temperature results in the production of more water.

In order to expand the research on adsorption desalting, this study attempted to increase the efficiency of such a technology via heat and mass recovery. There are also two new designs for mass and heat recovery that are quite different from the previous research on the advanced ADS. The purpose of heat recovery is to absorb the internal heat between the adsorption beds, and transfer it through the condenser to the evaporator. This allows the evaporator temperature, and then the evaporation rate, to increase, leading to the promotion of desalinated water production. On the other hand, the purpose of mass recovery is the transfer of pressure from the hot bed to the cold. The thermodynamic modeling of the adsorption desalination systems (ADS) under different operating conditions were investigated. Also, its effect on the evaporator vapor production and the water vapor adsorption and desorption in the adsorption beds were examined. The mathematical model of ADS thermodynamics was then validated with the experimental data. The advanced ADS modeling was also conducted via mass and heat recovery among beds, condensers and evaporators, and in addition to the amount of the desalinated water, the time history chart of the equipment applied in the process with and without the thermal recovery and mass was revealed. The cycle performance was evaluated in terms of daily specific water production (SDWP), specific cooling capacity (SCC), and coefficient of performance (COP). The recovery mode was new to this plan. This configuration could improve the ADS performance to a great extent.

The ADS cycle's configuration

Figure 1 shows the ADS design of the two beds with the mass and heat recovery designs in different modes. The

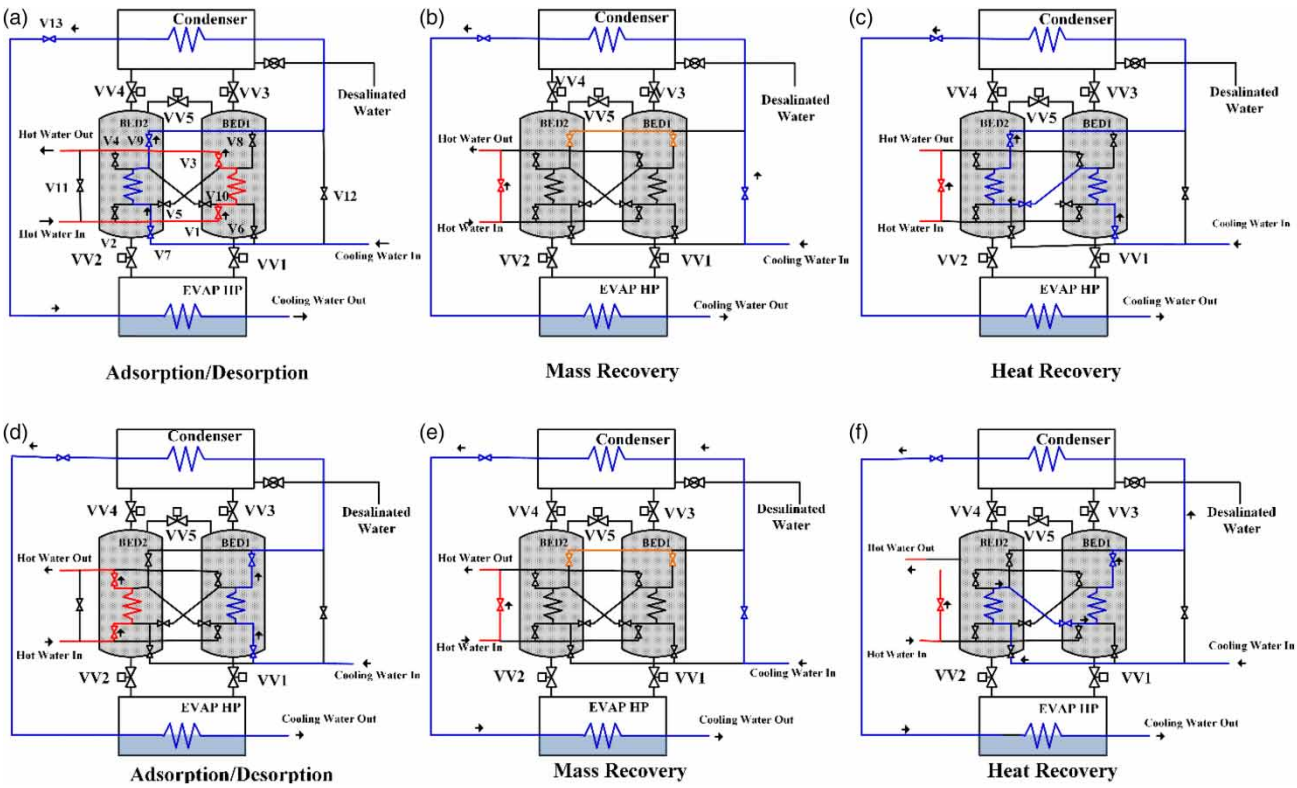

Figure 1 | Schematic design of the two-bed ADS in different modes.

Downloaded from http://iwaponline.com/jwrd/article-pdf/11/1/136/842416/jwrd0110136.pdf
by guest

system consists of an evaporator, two adsorption beds, and a condenser. In the first mode, bed 2 is in the adsorption mode and bed 1 is in the desorption mode. In this mode, thermal recovery operates between bed 2 and the condenser to evaporator. In the second mode, mass recovery, the two beds are connected to each other and the mass and pressure are transferred from the high temperature bed to the low temperature bed. In the third mode, the final thermal recovery is performed between the high temperature bed, the low temperature bed, and the condenser to the evaporator.

Mathematical modeling of ADS

Adsorption isotherm estimates the amount of the adsorbate adsorbed by the adsorbent at constant temperature versus pressure. The linear driving force (LDF) model states the transient uptake as below (Kim *et al.* 2014):

$$\frac{d\omega}{dt} = \frac{f_0 D_{so} \exp\left(\frac{-E_a}{RT}\right)}{R_p^2}(\omega^* - \omega) \tag{1}$$

Table 1 shows constant parameters in linear driving force (LDF) model for different materials.

Mass and energy balances equations

The equation of mass balance for each cycle is obtained by:

$$\frac{dM_{s,evp}}{dt} = \dot{m}_{s,in} - \dot{m}_{d,cond} - \dot{m}_b \tag{2}$$

Two-bed adsorption desalination works in three modes of the absorption/desorption, the mass and heat recovery. The energy balance during the adsorption/desorption mode can be written as follows:

$$(M_{sg}cp_{sg} + M_{cu}cp_{cu} + M_{al}cp_{al} + M_{sg}\,w\,cp_{g(T_{bed})})_{bed}\frac{dT_{bed}}{dt} = M_{sg}\frac{d\omega_{bed}}{dt}\,Q_{ST(T_{bed},\,P_{evap/cond})} - \dot{m}_{cw/hw}\,cp_{w(T_{bed})}(T_{cw/hw,out} - T_{cw/hw,in})_{bed} \tag{3}$$

The energy balance during the mass and heat recovery mode is given as below respectively:

$$(M_{sg}cp_{sg} + M_{cu}cp_{cu} + M_{al}cp_{al} + M_{sg}\,w\,cp_{g(T_{bed})})_{bed}\frac{dT_{bed}}{dt} = 0 \tag{4}$$

$$(M_{sg}cp_{sg} + M_{cu}cp_{cu} + M_{al}cp_{al} + M_{sg}\,w\,cp_{g(T\_bed)})_{bed}\frac{dT_{bed}}{dt} = -\dot{m}_{cw}\,cp_{cw(T_{bed})}(T_{cw,out} - T_{cw,in})_{bed} \tag{5}$$

The evaporator and condenser energy balance is given as below respectively:

$$(M_{s,evap}cp_{s(T_{evap})} + M_{hex,evap}cp_{hex})_{evap}\frac{dT_{evap}}{dt} = \dot{m}_{s,in}\,h_{f(T_{feed})} - M_{sg}\frac{dw_{ads}}{dt}\,h_{fg(T_{evap})} - \dot{m}_{cw,evap}\,cp_w(T_{cw,out} - T_{cw,in})_{evap} \tag{6}$$

$$(M_{cond}cp_{(T_{cond})} + M_{hex,cond}cp_{hex})_{cond}\frac{dT_{cond}}{dt} = -\frac{dM_d}{dt}\,h_{f(T_{cond})} + M_{sg}\frac{dw_{bed}}{dt}\,h_{fg(T_{cond})} - \dot{m}_{cw,cond}\,cp_{w(T_{cond})}(T_{cw,out} - T_{cw,in})_{cond} \tag{7}$$

The desorption, condensation and evaporation heat are derived by:

$$Q_{des} = \frac{1}{t_{cycle}}\int_0^{t_{cycle}} \dot{m}_{hw}cp_{hw(T_{hw})}(T_{hw,in-}T_{hw,out})dt$$

$$Q_{cond} = \frac{1}{t_{cycle}}\int_0^{t_{cycle}} \dot{m}_{w,cond}\,cp_{w(T_{cond})}(T_{w,cond,in} - T_{w,cond,out})dt \tag{8}$$

Finally, the system performance is evaluated by the Specific Daily Water Production (SDWP) and the performance ratio (PR).

$$SDWP = \int_0^{t_{cycle}} \frac{Q_{cond}\tau}{h_{fg(T_{cond})}M_{sg}}dt$$

$$PR = \int_0^{t_{cycle}} \frac{\dot{m}_d h_{fg(T_{cond})}\tau}{(Q_{des})}dt \tag{9}$$

Downloaded from http://iwaponline.com/jwrd/article-pdf/11/1/136/842416/jwrd0110136.pdf
by guest

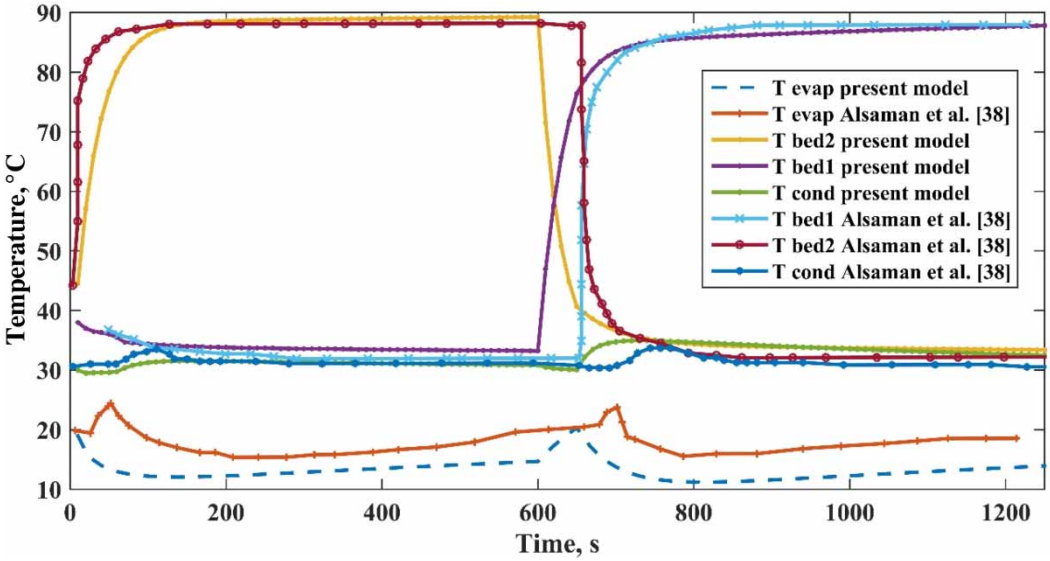

Figure 2 | Time history of temperatures of the ADS without mass and heat recovery that predicts by the present model against Alsaman *et al.*'s (2017) data.

Table 2 | AD cycle operating conditions (Alsaman *et al.* 2017)

Parameters	Value	Unit
Heat transfer coefficient of bed	600	W/K
Heat transfer coefficient of evaporator	350	W/K
Heat transfer coefficient of condenser	500	W/K
Fin of heat exchanger of bed weight	0.72	kg
Tube of heat exchanger of bed weight	2.97	kg
Tube of heat exchanger of evaporator weight	1.3	kg
Weight of silica gel	6.75	kg
Tube of heat exchanger of condenser weight	1.535	kg
Cycle time	650	s

RESULTS AND DISCUSSION

In this study, to validate the present ADS mathematical modeling, the temperatures of the main equipment were compared with Alsaman's *et al.* (2017) experimental results (Figure 2). Finally, ADS was proposed with an advanced mass and heat recovery design as shown in Table 2.

In Figure 3, the amount of water adsorbed in the adsorption beds with and without recovery state is shown in the adsorption cycles. Recovery mode includes heat recovery between the adsorption beds and the condenser

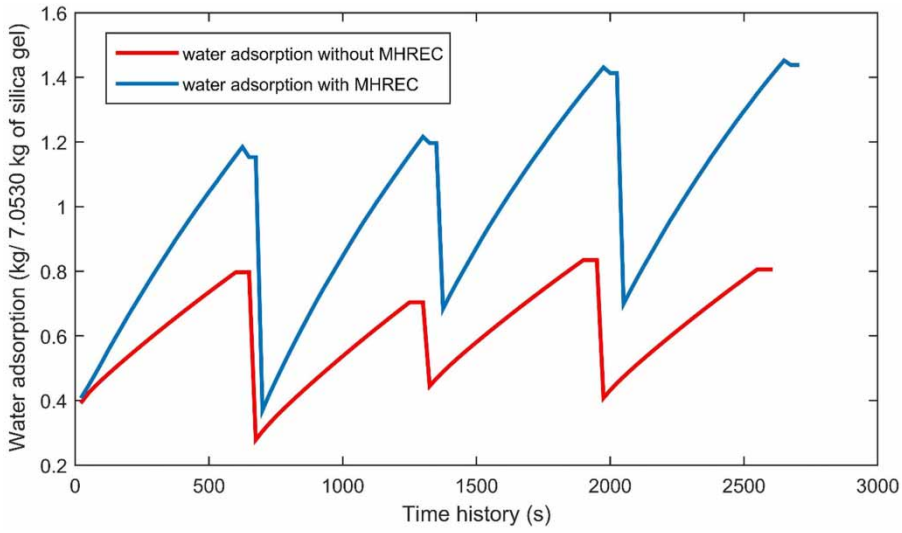

Figure 3 | Time history of water adsorption with and without mass and heat recovery.

Downloaded from http://iwaponline.com/jwrd/article-pdf/11/1/136/842416/jwrd0110136.pdf
by guest

to the evaporator, as well as mass recovery between the two beds. As shown in Figure 3, the first and third half cycles correspond to bed 1 and the second and fourth half cycles correspond to bed 2. In the recovery mode, the slope of the absorbed water diagram is greater than the one in the non-recovery mode, indicating that the adsorption rate is higher in the recovery mode. Figure 4 shows the time history of the bed-1 water uptake and offtake with and without mass and heat recovery. As can be seen in the diagram, the slope of the recovery mode is higher than the non-recovery mode.

Figure 5 illustrates the amount of water excreted in the adsorbed beds in the desorption state. As shown in the figure, the first and third half cycles are related to bed 2, and the second and fourth half cycles pertain to bed 1. In the first half cycle of bed 2, since the system has not produced the vapor yet, almost no vapor is excreted in the desorption mode. The slope of the recovery mode diagram

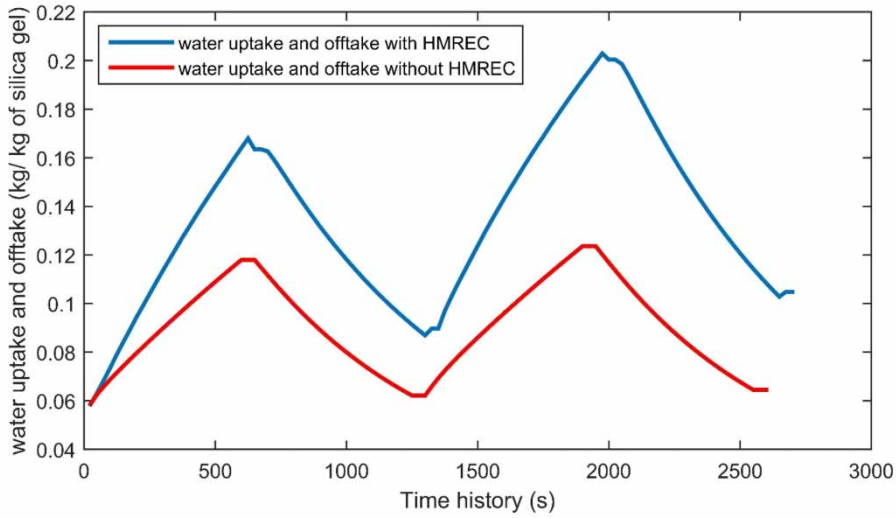

Figure 4 | Time history of bed-1 water uptake and offtake with and without mass and heat recovery.

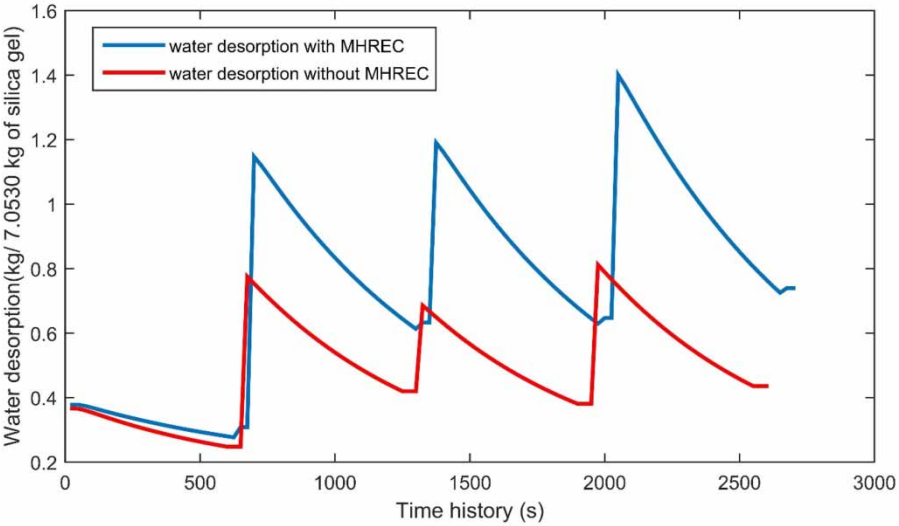

Figure 5 | Time history of water desorption with and without mass and heat recovery.

Downloaded from http://iwaponline.com/jwrd/article-pdf/11/1/136/842416/jwrd0110136.pdf
by guest

is higher than the one without the recovery mode, indicating that the amount of the water adsorbed, and ultimately the amount of the water produced, would be higher. Figure 6 shows the time history of the bed-2 water uptake and offtake with and without mass and heat recovery.

Figure 7 shows the reduction of seawater mass inside the evaporator versus the time without and with the mass and heat recovery. As the figure reveals, the amount of water reduction in the evaporator in the recovery mode is higher than in the non-recovery mode, and this issue indicates that, in this case, the amount of water produced would also be higher. As shown in the recovery mode, the evaporation rate decreases with an increase in seawater concentration. In the first two cycles, the mass of seawater decreases from 3 to 1.8 kg, while, in the next three cycles, its mass only decreases from 1.8 to 1.45 kg.

Figures 8 and 9 illustrate the temperature variations for the evaporator, condenser, and adsorption beds. As shown

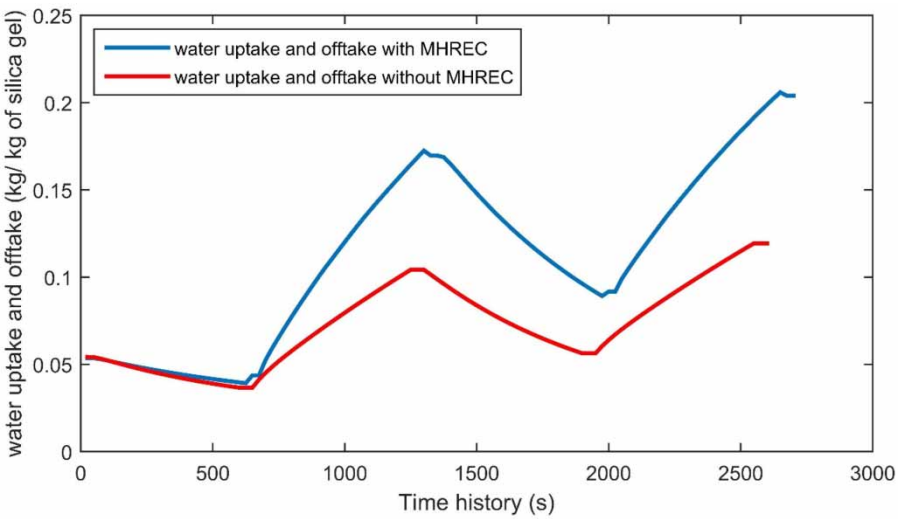

Figure 6 | Time history of bed-2 water uptake and offtake with and without mass and heat recovery.

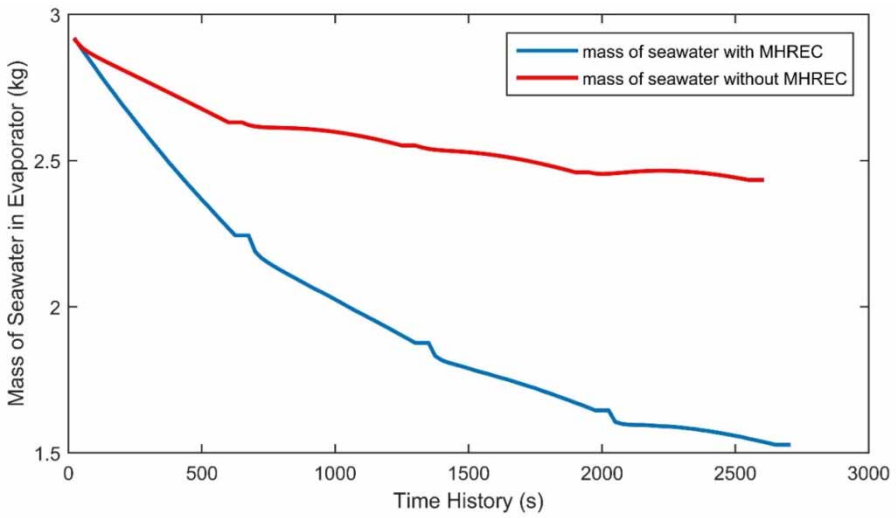

Figure 7 | Time history of seawater mass in evaporator with and without mass and heat recovery.

Downloaded from http://iwaponline.com/jwrd/article-pdf/11/1/136/842416/jwrd0110136.pdf
by guest

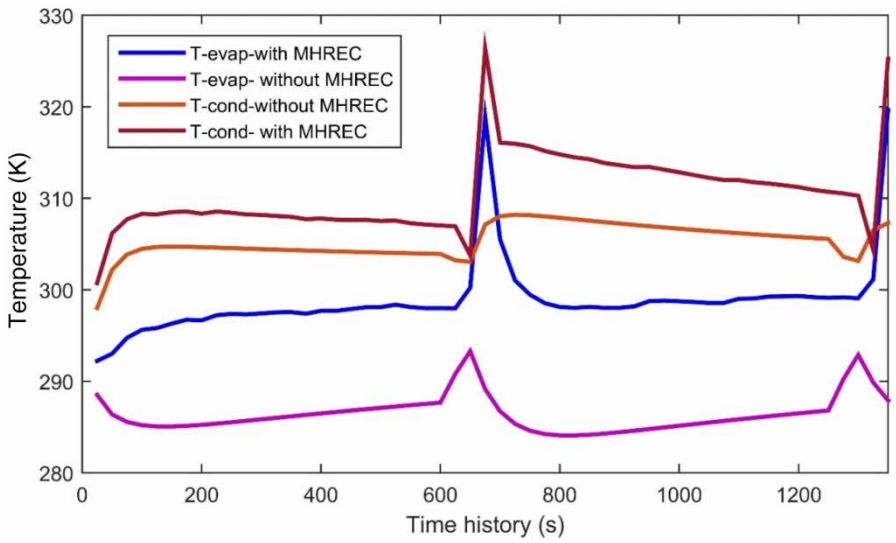

Figure 8 | Time history of temperatures for evaporator and condensor with and without mass and heat recovery.

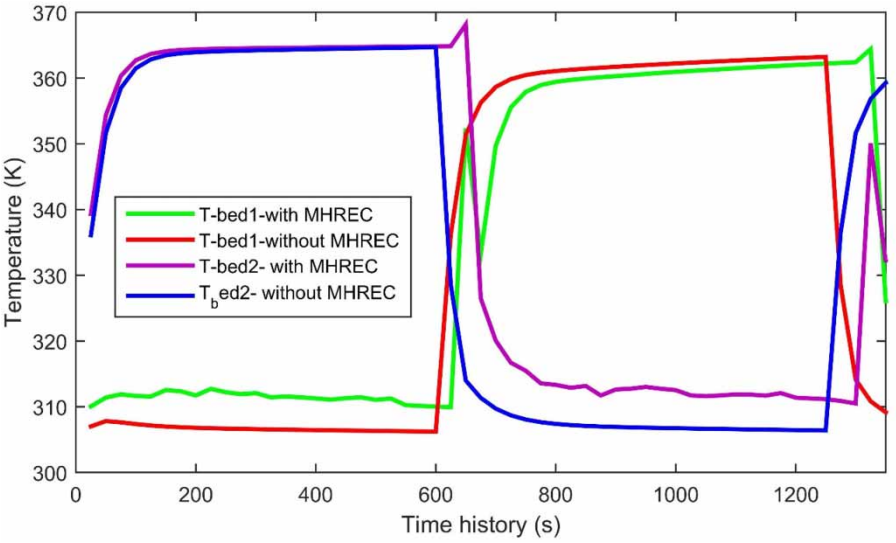

Figure 9 | Time history of temperatures for adsorption beds with and without mass and heat recovery.

in the figure, the mass and heat recovery leads to an increase in the temperature of the equipment and consequently an increase in the pressure. Increasing the temperature in the evaporator would promote the evaporation rate and at higher pressures the adsorbents are also more absorbable. Therefore, the amount of fresh water produced would be much higher than that of the conventional adsorption desalination.

Figure 10 shows the amount of desalinated water in different cycles. In the first cycle, the adsorption beds were free of the water vapor at first, therefore, the rate of desalinated water production was lower. Over time, and with the added mass and heat recovery effect, the amount of water produced became 14.37 m^3 per ton of silica gel. On the other hand, the amount of the water produced in Alsaman *et al.*'s (2017) study was 5.32 m^3 per ton of silica

Downloaded from http://iwaponline.com/jwrd/article-pdf/11/1/136/842416/jwrd0110136.pdf
by guest

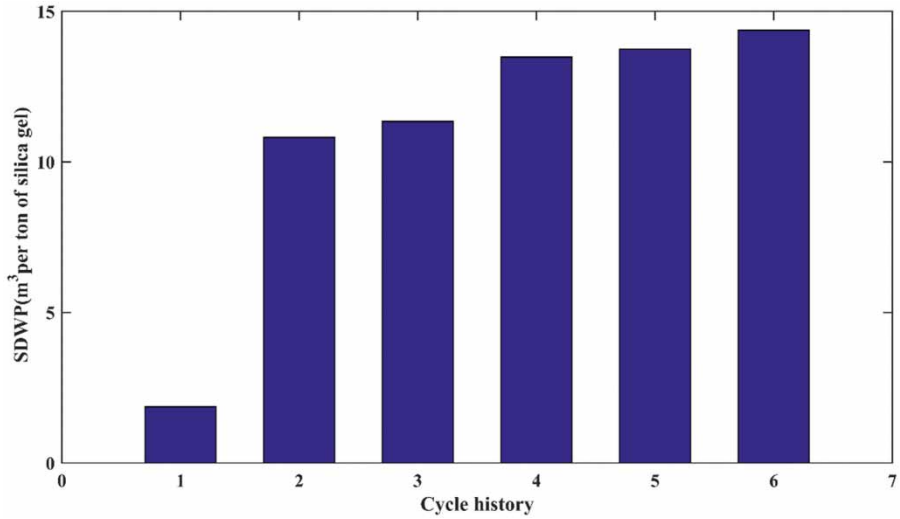

Figure 10 | SDWP at different cycle with mass and heat recovery.

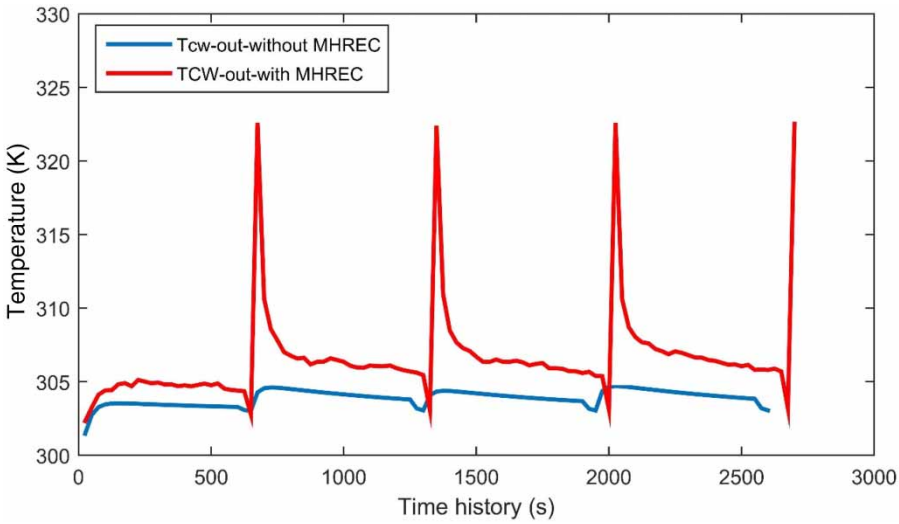

Figure 11 | Time history of temperatures of cooling water with and without mass and heat recovery.

gel at the hot water temperature of 92.5 °C. This increased rate of desalinated water production is due to the mass and heat recovery of the ADS process. It is worth noting that the fin pitch in the bed heat exchanger was assumed to be 4 mm.

Figure 11 elucidates the time history of the cooling water temperatures with and without the mass and heat recovery. As shown in the figure, the cold water temperature output from the system in the recovery mode is higher than in the non-recovery mode. This issue can be due to the transfer of the internal heat from the beds and the condenser to the evaporator.

CONCLUSIONS

In this study, a conventional ADS with heat and mass recovery cycles was modeled. The results indicated that the

Downloaded from http://iwaponline.com/jwrd/article-pdf/11/1/136/842416/jwrd0110136.pdf
by guest

prediction of SDWP by the present model had the same tendency as Alsaman *et al.*'s (2017) experimental data with quite acceptable accuracy. According to the results, the performance of the new ADS was significantly enhanced via heat and mass recovery among the beds, condenser, and evaporator. Also, the amount of water vapor produced in the evaporator and the amount of water vapor adsorption and desorption in the adsorption beds were shown. Besides, the effect of the heat and mass recovery on the equipment applied in the process revealed an excellent increase in the amount of desalinated water in the system. The maximum water production for this ADS was 14.37 m^3/1,000 kg of silica gel/day at the hot water temperature of 92.5 °C and the fin pitch of 4 mm. Consequently, the SDWP of the new ADS was 153% more than the conventional ADS. Certainly, the proper selection of temperature ranges, operating conditions, and time cycles can have a greater impact on the performance of the system.

ACKNOWLEDGEMENT

The authors wish to thank Hormozgan steel company (HOSCO) for sponsoring the project.

DATA AVAILABILITY STATEMENT

All relevant data are available from an online repository or repositories.

REFERENCES

Ali, S. M. & Chakraborty, A. 2016 Adsorption assisted double stage cooling and desalination employing silica gel+ water and AQSOA-Z02+ water systems. *Energy Conversion and Management* **117**, 193–205.

Alsaman, A. S., Askalany, A. A., Harby, K. & Ahmed, M. S. 2017 Performance evaluation of a solar-driven adsorption desalination-cooling system. *Energy* **128**, 196–207.

Amirfakhraei, A., Zarei, T. & Khorshidi, J. 2020 Performance improvement of adsorption desalination system by applying mass and heat recovery processes. *Thermal Science and Engineering Progress* **18**, 100516.

De Villiers, M. 2001 *Water: The Fate of Our Most Precious Resource*. Houghton Mifflin Harcourt, New York.

Garg, K., Khullar, V., Das, S. K. & Tyagi, H. 2019 Parametric study of the energy efficiency of the HDH desalination unit integrated with nanofluid-based solar collector. *Journal of Thermal Analysis and Calorimetry* **135** (2), 1465–1478.

Gleick, P. H. 1993 *Water in Crisis*. Pacific Institute for Studies in Dev., Environment & Security. Stockholm Env. Institute, Oxford University Press, Oxford, p. 473.

Hulton, G. & World Health Organization 2012 *Global Costs and Benefits of Drinking-Water Supply and Sanitation Interventions to Reach the MDG Target and Universal Coverage*. World Health Organization, Geneva, Switzerland.

Kaldellis, J. & Kondili, E. 2007 The water shortage problem in the Aegean archipelago islands: cost-effective desalination prospects. *Desalination* **216** (1–3), 123–138.

Karagiannis, I. C. & Soldatos, P. G. 2008 Water desalination cost literature: review and assessment. *Desalination* **223** (1–3), 448–456.

Kariman, H., Hoseinzadeh, S., Shirkhani, A., Heyns, P. S. & Wannenburg, J. 2019 Energy and economic analysis of evaporative vacuum easy desalination system with brine tank. *Journal of Thermal Analysis and Calorimetry* **140**, 1–10.

Kim, Y.-D., Thu, K., Masry, M. E. & Ng, K. C. 2014 Water quality assessment of solar-assisted adsorption desalination cycle. *Desalination* **344**, 144–151.

Miller, J. E. 2003 *Review of Water Resources and Desalination Technologies*. Sandia National Laboratories, Albuquerque, NM. 49, pp. 2003–0800.

Navarro, T. 2018 Water reuse and desalination in Spain – challenges and opportunities. *Journal of Water Reuse and Desalination* **8** (2), 153–168.

Ng, K. C., Thu, K., Kim, Y., Chakraborty, A. & Amy, G. 2013 Adsorption desalination: an emerging low-cost thermal desalination method. *Desalination* **308**, 161–179.

Sabiri, N.-E., Séchet, V., Jaouen, P., Pontié, M., Massé, A. & Plantier, S. 2018 Impact of granular filtration on ultrafiltration membrane performance as pre-treatment to seawater desalination in presence of algal blooms. *Journal of Water Reuse and Desalination* **8** (2), 262–277.

Sadi, M., Fakharian, H., Ganji, H. & Kakavand, M. 2019 Evolving artificial intelligence techniques to model the hydrate-based desalination process of produced water. *Journal of Water Reuse and Desalination* **9** (4), 372–384.

Seyednezhad, M., Sheikholeslami, M., Ali, J. A., Shafee, A. & Nguyen, T. K. 2020 Nanoparticles for water desalination in solar heat exchanger. *Journal of Thermal Analysis and Calorimetry* **139** (3), 1619–1636.

Shahzad, M. W., Ng, K. C., Thu, K., Saha, B. B. & Chun, W. G. 2014 Multi effect desalination and adsorption desalination (MEDAD): a hybrid desalination method. *Applied Thermal Engineering* **72** (2), 289–297.

Thomas, C. 1994 *Water in Crisis: A Guide to the World's Fresh Water Resources*. Oxford University Press, New York.

Downloaded from http://iwaponline.com/jwrd/article-pdf/11/1/136/842416/jwrd0110136.pdf
by guest

Thu, K., Saha, B. B., Chakraborty, A., Chun, W. G. & Ng, K. C. 2011 Study on an advanced adsorption desalination cycle with evaporator–condenser heat recovery circuit. *International Journal of Heat and Mass Transfer* **54** (1–3), 43–51.

Thu, K., Chakraborty, A., Kim, Y. D., Myat, A., Saha, B. B. & Ng, K. C. 2013a Numerical simulation and performance investigation of an advanced adsorption desalination cycle. *Desalination* **308**, 209–218.

Thu, K., Kim, Y. D., Myat, A., Chakraborty, A. & Ng, K. C. 2013b Performance investigation of advanced adsorption desalination cycle with condenser–evaporator heat recovery scheme. *Desalination and Water Treatment* **51** (1–3), 150–163.

Thu, K., Chakraborty, A., Saha, B. B. & Ng, K. C. 2013c Thermo-physical properties of silica gel for adsorption desalination cycle. *Applied Thermal Engineering* **50** (2), 1596–1602.

Thu, K., Kim, Y. D., Amy, G., Chun, W. G. & Ng, K. C. 2013d A hybrid multi-effect distillation and adsorption cycle. *Applied Energy* **104**, 810–821.

Thu, K., Yanagi, H., Saha, B. B. & Ng, K. C. 2013e Performance analysis of a low-temperature waste heat-driven adsorption desalination prototype. *International Journal of Heat and Mass Transfer* **65**, 662–669.

Thu, K., Kim, Y. D., Amy, G., Chun, W. G. & Ng, K. C. 2014 A synergetic hybridization of adsorption cycle with the multi-effect distillation (MED). *Applied Thermal Engineering* **62** (1), 245–255.

Tlili, I., Alkanhal, T. A., Othman, M., Dara, R. N. & Shafee, A. 2019 Water management and desalination in KSA view 2030. *Journal of Thermal Analysis and Calorimetry* **139**, 1–12.

Tokarev, M., Gordeeva, L., Romannikov, V., Glaznev, I. & Aristov, Y. 2002 New composite sorbent CaCl2 in mesopores for sorption cooling/heating. *International Journal of Thermal Sciences* **41** (5), 470–474.

Trenberth, K. E., Smith, L., Qian, T., Dai, A. & Fasullo, J. 2007 Estimates of the global water budget and its annual cycle using observational and model data. *Journal of Hydrometeorology* **8** (4), 758–769.

Wang, X., Ng, K. C., Chakarborty, A. & Saha, B. B. 2007 How heat and mass recovery strategies impact the performance of adsorption desalination plant: theory and experiments. *Heat Transfer Engineering* **28** (2), 147–153.

Wang, D., Zhang, J., Tian, X., Liu, D. & Sumathy, K. 2014 Progress in silica gel–water adsorption refrigeration technology. *Renewable and Sustainable Energy Reviews* **30**, 85–104.

Xu, D., Acker, T. & Zhang, X. 2019 Size optimization of a hybrid PV/wind/diesel/battery power system for reverse osmosis desalination. *Journal of Water Reuse and Desalination* **9** (4), 405–422.

Youssef, P., Al-Dadah, R. & Mahmoud, S. 2014 Comparative analysis of desalination technologies. *Energy Procedia* **61**, 2604–2607.

Youssef, P., Al-Dadah, R. K., Mahmoud, S. M., Dakkama, H. J. & Elsayed, A. 2015a Effect of evaporator and condenser temperatures on the performance of adsorption desalination cooling cycle. *Energy Procedia* **75**, 1464–1469.

Youssef, P. G., Mahmoud, S. M. & Al-Dadah, R. K. 2015b Performance analysis of four bed adsorption water desalination/refrigeration system, comparison of AQSOA-Z02 to silica-gel. *Desalination* **375**, 100–107.

Youssef, P. G., Mahmoud, S. M. & Al-Dadah, R. K. 2016 Numerical simulation of combined adsorption desalination and cooling cycles with integrated evaporator/condenser. *Desalination* **392**, 14–24.

Zarei, T. & Behyad, R. 2019 Predicting the water production of a solar seawater greenhouse desalination unit using multi-layer perceptron model. *Solar Energy* **177**, 595–603.

Zhu, Z., Peng, D. & Wang, H. 2019 Seawater desalination in China: an overview. *Journal of Water Reuse and Desalination* **9** (2), 115–132.

Zhu, D., Wu, H. & Wang, S. 2006 Experimental study on composite silica gel supported cacl2 sorbent for low grade heat storage. *International Journal of Thermal Sciences* **45** (8), 804–813.

First received 15 June 2020; accepted in revised form 26 October 2020. Available online 5 January 2021

Downloaded from http://iwaponline.com/jwrd/article-pdf/11/1/136/842416/jwrd0110136.pdf
by guest